

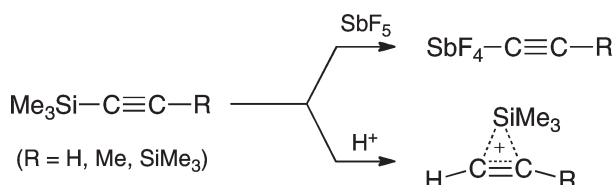
Reaction of Trimethylsilylacetylenes with Antimony Pentafluoride under Matrix Isolation Conditions: Experimental and Computational Study[†]

Helena Čičak, Hrvoj Vančik, and Zlatko Mihalić*

*Department of Chemistry, Faculty of Science,
University of Zagreb, Horvatovac 102a,
10000 Zagreb, Croatia*

mihalic@chem.pmf.hr

Received June 23, 2010

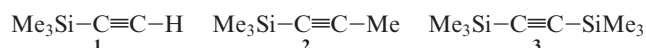


Reaction of trimethylsilylacetylenes $\text{Me}_3\text{SiC}\equiv\text{CR}$ with SbF_5 in the solid state was investigated using matrix isolation infrared spectroscopy and quantum-mechanical calculations. Two reaction pathways were detected. Replacement of the trimethylsilyl group with SbF_4 produces neutral antimony acetylides $\text{F}_4\text{SbC}\equiv\text{CR}$. Acetylenic bond protonation produces silyl cation **6-R**, fully bridged for $\text{R} = \text{H}$ and SiMe_3 . High total charges on the bridging SiMe_3 group and low $\text{Me}_3\text{Si}-\text{C}$ bond orders to acetylenic moiety, both calculated at the MP4(SDQ)/6-311G(d,p) level of theory, indicate high silyl cation character of these species.

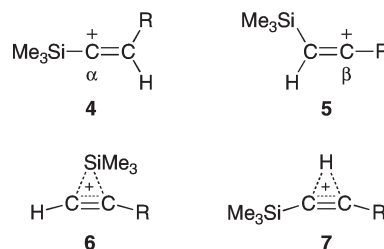
One of the challenging goals in organosilicon chemistry is isolation of free planar tricoordinated silyl cation in the

condensed phase, analogous to carbocations which have long been known and characterized as free species.¹⁻¹⁶ Although silyl cations are thermodynamically more stable than their carbon counterparts, at the same time they are very reactive due to their high inherent electrophilicity and ability to produce hypervalent coordination. Since smaller steric hindrance makes them more sensitive to solvation and other environmental effects, the observation of free silyl cations in the condensed phase proved to be very difficult. Most such species observed so far had more or less reduced degrees of silyl cation character.

In this paper, we report the isolation and silyl cation character of species formed by reactions of trimethylsilylacetylenes **1–3** with superacid SbF_5 in the solid state using matrix isolation infrared spectroscopy combined with quantum-mechanical calculations.^{17–19}



Under such conditions, bearing in mind that SbF_5 contains traces of moisture, it is reasonable to expect acetylenic bond protonation^{20,21} and formation of some of silyl vinyl cations **4–7** ($\text{R} = \text{H}, \text{Me}, \text{SiMe}_3$). Since all of them have vinyl stretching frequencies in the IR spectral region free from other vibrations, comparison of corresponding experimental and calculated frequencies should allow simple identification of formed species.



Experimental IR spectra of acetylenes **1–3** codeposited with SbF₅ at temperature of liquid nitrogen are given in Figure 1. In all three cases, immediately after deposition and later during matrix warming, new bands appear in the C≡C bond stretching spectral region. Since the protonation of the triple bond reduces its bond order, lower frequency bands

[†] Dedicated to the memory of Professor Emeritus Dionis E. Sunko (1922–2010).

(1) Apeloig, Y. In *The Chemistry of Organic Silicon Compounds*; Patai, S., Rappoport, Z., Eds.; John Wiley & Sons: New York, 1989; pp 57–225.

(2) Karni, M.; Apeloig, Y.; Kapp, J.; Schleyer, P. v. R. In *The Chemistry of Organic Silicon Compounds*; Rappoport, Z., Apeloig, Y., Eds.; John Wiley & Sons: New York, 2001; pp 77–122.

(3) Ottosson, C.-H.; Kraka, E.; Cremer, D. In *Pauling's Legacy: Modern Modelling of the Chemical Bond*; Maksić, Z. B., Orville-Thomas, W. J., Eds.; Theoretical and Computational Chemistry, Vol. 6; Elsevier Science B.V.: New York, 1999; pp 231–301.

(4) Prakash, G. K. S.; Keyaniyan, S.; Anisfeld, R.; Heiliger, L.; Olah, G. A.; Stevens, R. C.; Choi, H.-K.; Bau, R. *J. Am. Chem. Soc.* **1987**, *109*, 5123.

(5) Olah, G. A.; Rasul, G.; Heiliger, L.; Bausch, J.; Prakash, G. K. S. *J. Am. Chem. Soc.* **1992**, *114*, 7737.

(6) Schleyer, P. v. R.; Buzek, P.; Müller, T.; Apeloig, Y.; Siehl, H.-U. *Angew. Chem., Int. Ed. Engl.* **1993**, 32 (10), 1471.

(8) Lambert, J. B.; Kania, L.; Zhang, S. *Chem. Rev.* **1995**, 95, 1191.

(9) Olsson, L.; Ottosson, C.-H.; Cremer, D. *J. Am. Chem. Soc.* **1995**, *117*, 7460.

(10) Arshadi, M.; Johnels, D.; Edlund, U.; Ottosson, C.-H.; Cremer, D. *J. Am. Chem. Soc.* **1996**, *118*, 5120.

(11) Xie, Z.; Manning, J.; Reed, R. W.; Mathur, R.; Boyd, P. D. W.; Benesi, A.; Reed, C. A. *J. Am. Chem. Soc.* **1996**, *118*, 2922.

(12) Ottosson, C.-H.; Cremer, D. *Organometallics* **1996**, *15* (26), 5495.

(13) Belzner, J. *Angew. Chem., Int. Ed. Engl.* **1997**, 36 (12), 1277.

(14) Ottosson, C.-H.; Szabó, K. J.; Cremer, D. *Organometallics* **1997**, 16 (11), 2377.

(16) Xie, Z.; Bau, R.; Benesi, A.; Reed, C. A. *Organometallics* **1995**, *14* (8).

(17) Vančik, H.; Sunko, D. E. *J. Am. Chem. Soc.* **1989**, *111*, 3742–3744.

(19) Sunko, D. E. In *Stable Carbocation Chemistry*; Surya Prakash,

G. K., Schleyer, P. v. R., Eds.; John Wiley & Sons, Inc.: New York, 1996; pp 349–386.

(20) Gabelica, V.; Kresge, A. J. *J. Am. Chem. Soc.* **1996**, *118* (16), 3838–3841.

(21) Kresge, J.; Tobin, J. B. *Angew. Chem., Int. Ed. Engl.* **1993**, 32 (5), 721-723.

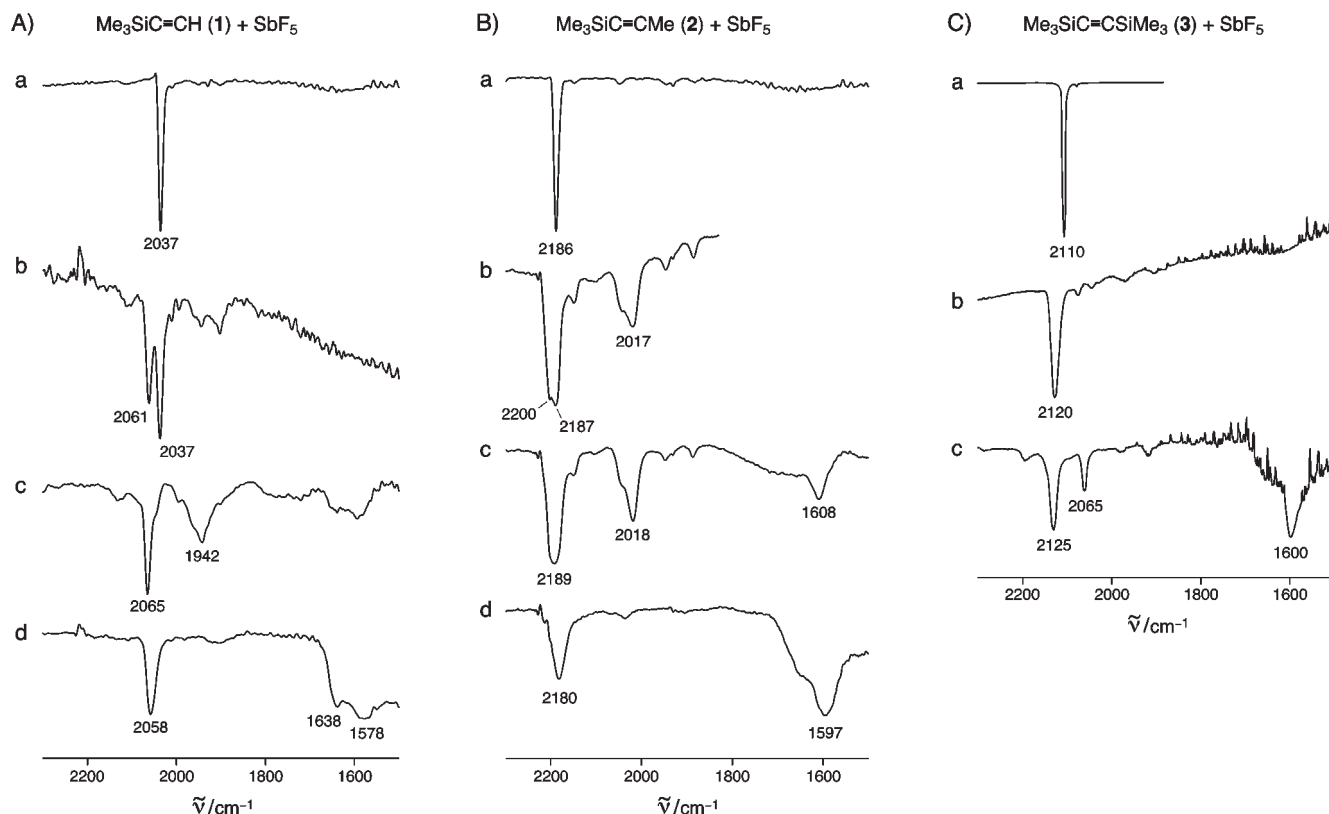
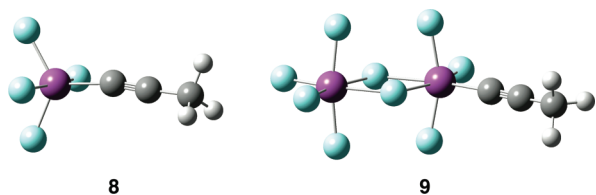


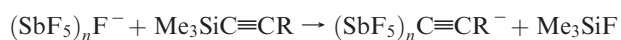
FIGURE 1. (A) IR spectra of $\text{Me}_3\text{SiC}\equiv\text{CH}$ (a) at room temperature, (b) after codeposition with SbF_5 at 77 K, and (c, d) during matrix warming from 77 K to rt. (B) IR spectra of $\text{Me}_3\text{SiC}\equiv\text{CMe}$ (a) at rt, (b) after codeposition with SbF_5 at 77 K, and (c, d) during matrix warming from 77 K to rt. (C) (a) Raman spectra of $\text{Me}_3\text{SiC}\equiv\text{CSiMe}_3$ at rt, (b) IR spectra of $\text{Me}_3\text{SiC}\equiv\text{CSiMe}_3$ after codeposition with SbF_5 at 77 K, and (c) during matrix warming from 77 K to rt.

can be ascribed to already mentioned cationic species or species formed by their rearrangements.

On the other hand, appearance of new higher frequency bands at first looks unusual. The case of symmetrical 1,2-bis-(trimethylsilyl)acetylene (**3**) provides the key to understanding reactions that take place. Immediately after the deposition, a new band in the IR spectrum of **3** appears, 10 cm^{-1} higher than its Raman $\text{C}\equiv\text{C}$ stretching frequency, indicating facile formation of compound with nonsymmetrically substituted triple bond. We suggest that in all three cases trimethylsilylacetylenes react with SbF_5 producing species with a $\text{Sb}-\text{C}$ bond, similar to **8** or **9**.



Calculations at the MP2(fc)/6-311+G(d,p) level of theory demonstrated that the reactions of trimethylsilylacetylenes **1–3** with $(\text{SbF}_5)_n$ or $(\text{SbF}_5)_n\text{F}^-$ ($n = 1$ or 2), producing Me_3SiF and neutral or negatively charged species containing a $\text{RC}\equiv\text{C}$ group bonded to antimony, are exothermic in all of the examined cases.



For the same R, reaction energies almost do not depend on the value of n . For the different R's, energies for the first reaction vary between -17 and -21 kcal/mol and for the second one between -1.7 and -6.6 kcal/mol , suggesting preferential formation of neutral species. There are almost no differences in calculated triple bond stretching frequencies between $\text{SbF}_4\text{C}\equiv\text{CR}$ and $\text{Sb}_2\text{F}_9\text{C}\equiv\text{CR}$, and most importantly, calculated frequencies are in a good agreement with the tentatively assigned experimental values (Table 1).

NBO analysis at the MP2(fc)/6-311+G(d,p) level of theory showed that $\text{Sb}-\text{C}$ bond in these compounds has bond order of 0.95 , 55% ionic character, and total charge of -0.51 on the $\text{C}\equiv\text{CR}$ group. Interestingly, these values are very similar to values obtained for the $\text{Si}-\text{C}(\equiv\text{C})$ bond in compounds **1–3** (0.99 , 50% , and -0.48 , respectively).

In conclusion, the examined trimethylsilylacetylenes **1–3** react with SbF_5 producing $\text{SbF}_4\text{C}\equiv\text{CR}$ (or $\text{Sb}_2\text{F}_9\text{C}\equiv\text{CR}$). Bands at 2063 cm^{-1} in the case of **1** and 2200 cm^{-1} in the case of **2** can be ascribed to $\text{C}\equiv\text{C}$ stretching vibrations of $\text{SbF}_4\text{C}\equiv\text{CH}$ and $\text{SbF}_4\text{C}\equiv\text{CMe}$, respectively. However, the reaction of **3** with SbF_5 is somewhat more complex. As initially produced $\text{SbF}_4\text{C}\equiv\text{CSiMe}_3$ (2120 cm^{-1}) gradually disappears, a new band appears at 2065 cm^{-1} , i.e., at the same frequency as the band assigned to $\text{C}\equiv\text{C}$ stretching of $\text{SbF}_4\text{C}\equiv\text{CH}$. Plausible explanation is that initially formed $\text{SbF}_4\text{C}\equiv\text{CSiMe}_3$ in the second step undergoes acid catalyzed desilylation, producing the same compound ($\text{SbF}_4\text{C}\equiv\text{CH}$) as does the direct reaction of **1** with SbF_5 . One cannot exclude the parallel formation of double substitution product,

TABLE 1. Average Experimental Wavenumbers of Bands in 2200–1900 cm^{-1} IR Spectral Region after Deposition, Corresponding Scaled^a Values Calculated at B3LYP/6-311G(d,p), MP2(fc)/6-311G(d,p), and MP4(sdq)/6-311G(d,p) Levels of Theory and Assigned Species^b

R	exptl	B3LYP	MP2	MP4	species
H	2037	2050	2005	2029	$\text{Me}_3\text{SiC}\equiv\text{CH}$
	2063	2070	2040		$\text{SbF}_4\text{C}\equiv\text{CH}$
	1942	1948	1913	1932	6-H
Me	2186	2173	2166	2169	$\text{Me}_3\text{SiC}\equiv\text{CMe}$
	2200	2187	2197		$\text{SbF}_4\text{C}\equiv\text{CMe}$
	2018	1986	2087	2027	6-Me
SiMe_3	2110 ^c	2106	2057		$\text{Me}_3\text{SiC}\equiv\text{CSiMe}_3$
	2120	2118	2088		$\text{SbF}_4\text{C}\equiv\text{CSiMe}_3$
	2065	2070	2040		$\text{SbF}_4\text{C}\equiv\text{CH}$

^aScaling formulas given in Supporting Information. ^bAverage rms deviation of all measured wavenumbers is about 6 cm^{-1} . ^cValue from Raman spectra.

$\text{F}_4\text{SbC}\equiv\text{CSbF}_4$, which cannot be detected because it does not have a $\text{C}\equiv\text{C}$ stretching band in the IR spectrum.

As already mentioned, bands with frequencies lower than the $\text{C}\equiv\text{C}$ stretching frequencies of parent acetylenes **1–3** can be tentatively ascribed to cationic species. Primarily, these are the 1942 cm^{-1} band in the case of compound **1** and the 2018 cm^{-1} band in the case of compound **2**. In some of the spectra collected during deposition of **3**, weak short-lived bands were observed in the same region, but they were not reproducible enough for serious consideration. With rising temperature, 1942 and 2018 cm^{-1} bands gradually disappear, and in all three cases new bands appear in the 1600 cm^{-1} region.

To identify the corresponding species, we conducted an exhaustive search for minima on potential energy surfaces belonging to the protonated trimethylsilylacetylenes **1–3**, using B3LYP/6-311G(d,p) and MP2(FC)/6-311G(d,p), two levels of theory often used in carbocation chemistry. In almost all of the cases the most stable unarranged structure is bridged cation **6**, 7–16 kcal/mol more stable than the second most stable one, which at the B3LYP level is α -silyl vinyl cation **4**, and at the MP2 level hydrogen-bridged cation **7**. The only exception is protonation of acetylene **3**, where B3LYP predicts the β -silyl cation **5** to be 1.2 kcal/mol more stable than cation **6**. There are numerous other differences between the results obtained by this two methods, with the common characteristics that MP2 structures have a higher degree of bridging than the corresponding B3LYP structures. Such a behavior was known previously and is generally indicative of flat regions of potential energy surfaces.²²

While at both levels of theory structure **6-H** has the calculated $\text{C}\equiv\text{C}$ stretching frequency close enough to the experimental value of 1942 cm^{-1} , corresponding frequencies of **6-Me** significantly differ from the 2018 cm^{-1} value found in the spectra of **2** (Table 1). For that reason, we decided to use a higher correlated method and reoptimized all of the structures located thus far at the MP4(SDQ)/6-311G(d,p)

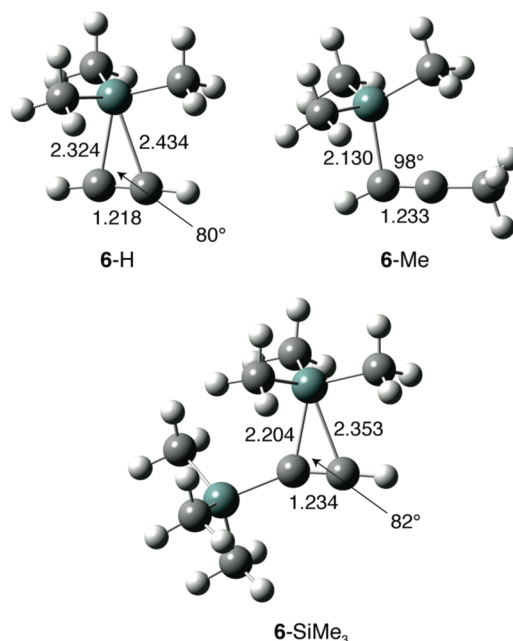


FIGURE 2. Geometries of silyl cations **6-R** (R = H, Me, SiMe_3) fully optimized at MP4(SDQ)/6-311G(d,p) level of theory (bond lengths in Å).

level of theory.²³ It turned out that the MP4 potential energy surface is simpler than the other two surfaces. Some of the shallow minima disappeared, and the bridged cation **6** is 8–11 kcal/mol more stable than the other unarranged structures. The optimized geometries of **6** are shown in Figure 2.

Since the MP4 $\text{C}\equiv\text{C}$ stretching vibration frequencies of both **6-H** and **6-Me** are in excellent agreement with the experimental values, we can safely conclude that under our experimental conditions acetylenic bond protonation of **1** and **2** initially leads to the bridged structure **6**.

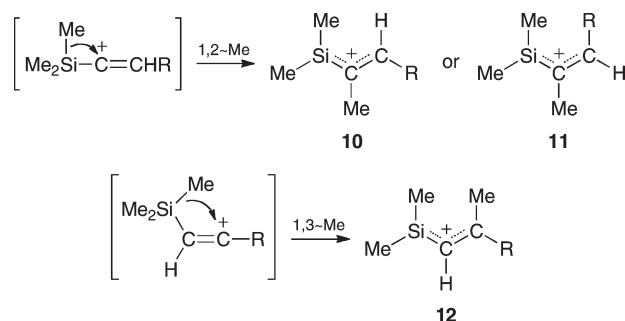
While **6-H** and **6-SiMe3** cations are fully bridged, the degree of bridging in **6-Me** is smaller, but significant. The geometric parameters alone indicating the nature of these silyl cations are convincing: small Si– $\text{C}\equiv\text{C}$ angles (symmetrically bridged **6-H** would have angle of about 75°), elongated Si–C bonds (corresponding bonds in **1–3** are in the 1.842–1.850 Å range), and only slightly changed $\text{C}\equiv\text{C}$ bond lengths in comparison to the ones in **1–3** (1.221–1.231 Å). Likewise, high NBO charges on the bridging SiMe_3 group (0.70–0.76) and low bridging Si–C NBO bond orders (0.03–0.09 except 0.31 for shorter bond in unsymmetrical **6-Me**) also indicate high silyl cationic character of these cations.

There are two possible explanations for the appearance of the new bands in the 1600 cm^{-1} spectral region. The most stable species located on all three levels of theory are various silaallyl cations (**10–12**), which can be formed by methyl shifts from initially formed protonated species (Scheme 1). As the calculated allyl group stretching frequencies of silaallyl cations belong to the same range of frequencies (1660–1580 cm^{-1}), it is reasonable to assume that such reactions indeed take place. However, one cannot ignore the possibility that these bands actually belong to fluoroalkenes formed by addition of HF to the acetylenic bond, since these

(22) (a) Vinković Vrček, I.; Vrček, V.; Siehl, H.-U. *J. Phys. Chem. A* **2002**, *106*, 1604–1611. (b) Fărcașiu, D.; Lukinskas, P.; Pamidighantam, S. V. *J. Phys. Chem. A* **2002**, *106*, 11672–11675. (c) Tantillo, D. J.; Pradeep, G. *Angew. Chem., Int. Ed.* **2005**, *44*, 2719–2723. (d) Siebert, M. R.; Tantillo, D. J. *J. Org. Chem.* **2006**, *71*, 645–654. (e) Bojin, M. D.; Tantillo, D. J. *J. Phys. Chem. A* **2006**, *110*, 4810–4816. (f) Mackie, I. A.; Govindhakannan, J.; DiLabio, G. A. *J. Phys. Chem. A* **2008**, *112*, 4004–4010.

(23) We have also tested QCISD and CCSD methods, using the same basis set, and the obtained results are in accord with the MP4(SDQ) results. We intend to discuss the potential energy surfaces of protonated trimethylsilylacetylenes in details in a full paper to be submitted.

SCHEME 1



compounds also have C=C stretching frequencies in this very region of the IR spectra.

Experimental Section

All reagents were p.a. grade commercially available chemicals.

Matrix isolation experiments were performed by standard techniques using a closed cycle cryostat cooled by liquid nitrogen and connected to the vacuum line.^{17–19} Matrices were prepared on a CsI window at 77 K and vacuum of 10^{-3} Torr. Used flasks were previously evacuated, and gaseous trimethylsilylacetylenes and SbF_5 codeposited at the volume ratio of approximately 1:5. Their mixing and deposition speed was regulated by specially constructed valve with magnetic gate programmed to open at desired time intervals. In all of the experiments, prior to evaporation, SbF_5 was briefly allowed to come into contact with air and thus acquire some moisture, later serving as source of protons.

Changes in the IR spectrum brought about by gradual warming of the matrix up to the room temperature were followed by a Perkin-Elmer 1725x FTIR spectrometer at 2 cm^{-1} resolution in the range of $1000\text{--}4000\text{ cm}^{-1}$.

Computational Details

The geometry of all of the examined species were fully optimized at MP2(fc)/6-311G(d,p) and B3LYP/6-311G(d,p) levels of theory using tight convergence criteria and, in the case of B3LYP calculations, more accurate numerical integration grid (int = ultrafine). In the case of species containing Sb, the LanL2DZdp ECP basis set^{24,25} was used for Sb atom(s). At each stationary point frequency calculation was performed at the same level of theory, both to characterize the geometry either as a minimum or a saddle point and to compare the calculated

frequencies with the experimental values. The most interesting minima were also reoptimized at the MP4(SDQ)/6-311G(d,p) level of theory, and afterward, frequencies were calculated at the same level of theory.

All of the reported energies in this paper are zero-point vibrational energy (ZPVE) corrected, using appropriate scaling factors.²⁶

To find a reliable way of comparing calculated and experimental frequencies, we have compared known frequencies of 19 neutral compounds and ions having multiple CC bond stretching frequencies in the $1600\text{--}2400\text{ cm}^{-1}$ spectral region, including five trimethylsilylacetylenes,²⁷ eight acetylenes and diacetylenes,²⁸ four allyl cations,^{29–31} 2-propenyl cation,³⁰ and acetylide anion,³² with the corresponding calculated values. At all levels of theory used, linear relationships were detected, with very good correlation parameters for the B3LYP ($s = 18\text{ cm}^{-1}$, $F = 4937$) and MP4(SDQ) ($s = 18\text{ cm}^{-1}$, $F = 3708$) frequencies and not as good for MP2(fc) frequencies ($s = 37\text{ cm}^{-1}$, $F = 919$). The obtained relationships (see the Supporting Information) were then used for scaling of appropriate calculated stretching frequencies of all found minimum energy species.

All of the calculations were carried out with the Gaussian 09 program,³³ except NBO/NRT analyses, which were performed with the NBO 5.0 module³⁴ embedded into the Gaussian 03 program.³⁵

Acknowledgment. This work was financially supported by the Ministry of Science, Education and Sports of The Republic of Croatia (Grant Nos. 119-1191342-1334 and 119-1191342-1339). The calculations were performed by using the CARNet Cruncher service of Croatian Academic and Research Network (CARNet).

Supporting Information Available: Computational methods, total energies, Cartesian coordinates, and vibrational frequencies. This material is available free of charge via the Internet at <http://pubs.acs.org>.

(24) (a) Hay, P. J.; Wadt, W. R. *J. Chem. Phys.* **1985**, *82*, 299. (b) Check, C. E.; Faust, T. O.; Bailey, J. M.; Wright, B. J.; Gilbert, T. M.; Sunderlin, L. S. *J. Phys. Chem. A* **2001**, *105*, 8111–8116.

(25) (a) Feller, D. *J. Comput. Chem.* **1996**, *17* (13), 1571–1586. (b) Schuchardt, K. L.; Didier, B. T.; Elsethagen, T.; Sun, L.; Gurumoorathi, V.; Chase, J.; Li, J.; Windus, T. L. *J. Chem. Inf. Model.* **2007**, *47* (3), 1045–1052.

(26) Merrick, J. P.; Moran, D.; Radom, L. *J. Phys. Chem. A* **2007**, *111*, 11683–11700.

(27) Values determined in this paper.

(28) NIST Computational Chemistry Comparison and Benchmark Database, NIST Standard Reference Database Number 101, Release 15a, April 2010; Johnson, R. D., III, Ed. <http://cccbdb.nist.gov/>.

(29) Buzek, P.; Schleyer, P. v. R.; Vančik, H.; Mihalić, Z.; Gauss, J. *Angew. Chem., Int. Ed. Engl.* **1994**, *33*, 448–451.

(30) Douberly, G. E.; Ricks, A. M.; Schleyer, P. v. R.; Duncan, M. A. *J. Chem. Phys.* **2008**, *128*, 021102.

(31) Kidemet, D.; Mihalić, Z.; Novak, I.; Vančik, H. *J. Org. Chem.* **1999**, *64*, 4931–4934.

(32) Ervin, K. M.; Lineberger, W. C. *J. Phys. Chem.* **1991**, *95*, 1167.

(33) *Gaussian 09, Revision A.02*; Frisch, M. J. et al., Gaussian, Inc.: Wallingford, CT, 2004.

(34) *NBO 5.0*; Glendening, E. D.; Badenhoop, J. K.; Reed, A. E.; Carpenter, J. E.; Bohmann, J. A.; Morales, C. M.; Weinhold, F. Theoretical Chemistry Institute, University of Wisconsin, Madison, 2001.

(35) *Gaussian 03, Revision E.01*; Frisch, M. J. et al., Gaussian, Inc.: Wallingford, CT, 2004.